Monatshefte für Chemie 132, 1413–1432 (2001)

Monatshefte für Chemie
Chemical Monthly

Invited Review

Phase Transitions and Critical Behaviour of Binary Liquid Mixtures

Gerhard Kahl*, **Elisabeth Schöll-Paschinger,** and **Andreas Lang**

Institut für Theoretische Physik und Center for Computational Materials Science, TU Wien, A-1040 Wien, Austria

Summary. Compared to the simple one-component case, the phase behaviour of binary liquid mixtures shows an incredibly rich variety of phenomena. In this contribution we restrict ourselves to so-called binary symmetric mixtures, *i.e.* where like-particle interactions are equal ($\Phi_{11}(r) = \Phi_{22}(r)$), whereas the interactions between unlike fluid particles differ from those of likes ones ($\Phi_{11}(r) \neq \Phi_{12}(r)$). Using both the simple mean spherical approximation and the more sophisticated self-consistent *Ornstein-Zernike* approximation, we have calculated the structural and thermodynamic properties of such a system and determine phase diagrams, paying particular attention to the critical behaviour (critical and tricritical points, critical end points). We then study the thermodynamic properties of the same binary mixture when it is in thermal equilibrium with a disordered porous matrix which we have realized by a frozen configuration of equally sized particles. We observe – in qualitative agreement with experiment – that already a minute matrix density is able to lead to drastic changes in the phase behaviour of the fluid. We systematically investigate the influence of the external system parameters (due to the matrix properties and the fluid–matrix interactions) and of the internal system parameters (due to the fluid properties) on the phase diagram.

Keywords. Binary fluid mixtures; Fluids in porous media; Phase transitions; Phase stability; Critical behaviour.

Introduction

The phase behaviour and the critical phenomena encountered in binary mixtures are considerably more complex than in the case of a pure fluid. Following the *Gibbs* rule, up to four phases can be observed simultaneously, and the way these phases can coexist often leads to rather complex phase diagrams. The phase behaviour is mainly triggered by two mechanisms (and their interrelation): first, there is the size difference of the particles of the two components and their (partial) penetrability; second, there is the chemical influence, expressed *via* the set of the three interatomic potentials, *i.e.* the interaction potentials between particles of the same species and the cross interaction between the unlike particles. The reader might get an impression of the complexity of the phase behaviour of a binary

* Corresponding author. E-mail: gkahl@tph.tuwien.ac.at

mixture from the review article of *Konynenburg* and *Scott* [1]: using a simple *van der Waals* model (which incorporates all relevant aspects of a binary mixture), these authors have classified several types of phase diagrams that can be encountered for such a system.

In this contribution we consider only a simplified version of a binary fluid mixture, which is usually called symmetric binary mixture in the literature. It is characterized by the fact that all particles are of the same size (ignoring thus the influence of particle size on the phase behaviour mentioned above). Further, the interactions between like particles are equal, only the unlike interaction (between particles of different species) is different. If we denote the fluid particles of the two species by indices '1' and '2', the set of interactions for a symmetric binary mixture are thus given by $\Phi_{11}(r) = \Phi_{22}(r) \neq \Phi_{12}(r)$. To further simplify the model, we assume the same functional form for all interatomic potentials; hence, $\Phi_{12}(r) = \alpha\Phi_{11}(r)$, α being different from 1. We additionally demand that our system be homogeneous and isotropic; therefore, potentials and the correlation functions (introduced later) are functions of the distance only. For such a system we will expect – apart from solid phases, which are not considered in this contribution – three different phases: the homogeneous equimolar gas phase (G), the homogeneous equimolar liquid (L), and the nonequimolar (demixed) fluid (DF), which consists itself of two coexisting phases, a 1-rich and a 2-rich fluid. Due to the symmetry, these two fluids have the same density. For $\alpha > 1$, where the unlike particle attraction dominates the like one, it is energetically more favourable for the mixture to exist in the equimolar phase; here we only expect a G-L transition (similar to that encountered in the one-component case), and no DF will be observed. In this contribution we have considered the more interesting case, *i.e.* $\alpha < 1$, where we expect both a G-L transition (as in the one-component case) and a demixing transition as well as the interplay of these two transitions.

The symmetry of our system leads to a reduction of types of phase diagrams that we encounter [2]: we observe three different archetypes which are distinguished by the location where the so-called λ-line (*i.e.* the critical line of the fluid demixing transition) intersects the first order G-L coexistence curve. In type I, where the λ-line meets the G-L coexistence curve well below the G-L critical point, we observe a critical end point (CEP) behaviour. In type II we observe a triple point (coexistence of G-, L-, and DF-phase) and a tricritical point (where an equimolar liquid, a 1-rich, and a 2-rich fluid become simultaneously critical); this point is characterized by two vanishing order parameters, the difference in the densities of the equimolar liquid and the DF-phase, and the difference in the concentrations of the two coexisting DF-phases. Type III is characterized again by a tricritical point; however, the G-L transition is suppressed. The variation $\mathrm{I} \to \mathrm{II} \to \mathrm{III}$ turns out to be induced by decreasing α.

In the second part of the present contribution we investigate this system when it is in thermal equilibrium with a disordered porous matrix of immobile particles, realized in our case by a frozen liquid configuration of particles of the same size as the fluid particles. Investigations of fluids that are in equilibrium with a disordered matrix have become a very challenging field in liquid-state physics during the past years [3]. Experimental and theoretical studies revealed that a porous matrix (even if it occupies only a minute fraction of the volume) can have a substantial influence

on the phase behavior of the liquid: ^{4}He and N_2 in high-porosity aerogel [4] are two examples where the near-critical liquid–vapor (LV) curve is narrowed drastically under the influence of a matrix. The effects become of course more interesting in the case that the fluid is a binary mixture; for example, experiments on a ^{3}He-^{4}He mixture inside a highly porous silica-gel or a porous gold matrix have shown a drastic modification of the superfluid transition [5]. A deeper understanding of these obviously very complex effects is all the more desirable as it might help to predict properties of materials of technological relevance (with widespread applications in catalysis, adsorption, *etc*.); for an overview, see Refs. [3, 6, 7].

Our simple model mimics the characteristic features of the matrix–fluid and fluid–fluid interaction of realistic systems and hence is able to give (at least qualitative) information of how a variation of the system parameters influences the phase behaviour. We present results of systematic variations of the system parameters and their influence on the phase behaviour of these complex systems. At this occasion one should point out that similar archetypes of phase diagrams (and sequences of these) are encountered in systems with completely different interatomic potentials: as examples we list here the *Heisenberg* fluid [8] (a fluid where the particles interact *via* hard-core and a *Heisenberg*-type interaction of their magnetic moments) and the *Stockmayer* fluid [9] (a fluid where the particles carry dipolar moments and interact – in addition – *via Lennard-Jones* potentials). In contrast to the present system, however, the changes between the three types of phase diagrams in these two examples are triggered by only one parameter.

In our calculations we have used liquid-state theories that are based on statistical mechanics for both systems. The central equations are the *Ornstein-Zernike* (OZ) equations [10] that relate the correlation functions of the particles of different species. For the binary case, the OZ-equations are three coupled integral-equations for the sets of correlation functions, each of them consisting of three functions. These equations are supplemented with a so-called closure relation that relates these functions with the set of pair potentials. In this contribution we have used the simple (and thermodynamically inconsistent) mean spherical approximation (MSA) [11] and the rather sophisticated (and thermodynamically self-consistent) self-consistent *Ornstein-Zernike* approximation (SCOZA) [12]. Despite its simplicity, the MSA model is able to give qualitative results for the phase diagram; thus, systematic trends can be worked out on a qualitative basis. However, this approach fails near the critical region: it is neither able to locate the critical point, nor is it able to give the correct critical exponents. The more refined SCOZA technique, on the other hand, gives highly accurate results for the phase boundaries and remains accurate as one approaches the critical region; its application is, however, restricted to the case of the bulk fluid as a consequence of the complexity of its concepts.

We have applied both methods to the case of the bulk fluid. We have investigated the influence of the interaction parameter α on the phase behaviour employing the MSA method, showing that the transition between the types of phase diagrams can be triggered by this parameter. Hence, in this investigation we refine in a quantitative way a study that was based on a simple mean field approach [2]. The MSA permits in addition, to identify metastable transitions that might be of relevance when studying dynamic processes. Using the SCOZA we have studied the stability of this fluid both with respect to mechanical and to chemical aspects.

The situation is much more delicate for the system where the fluid is in thermal equilibrium with the porous matrix. Here, a special approach *via* the so-called replica trick (explained in more detail below) has to be used: the concept (introduced to liquid-state physics by *Given* and *Stell* [13]) allows to map the system 'fluid + matrix' (which represents a very special three-component system) onto the limiting case of a fully equilibrated fluid mixture built up by the matrix and s identical and non-interacting copies of the fluid; thermodynamic and structural properties of the partly quenched original system ('fluid + matrix') are then obtained by taking the $(s \to 0)$-limit of the corresponding quantities of the fully equilibrated replicated system. The formalism arising from this route is rather complex even for a simple closure relation like the MSA (for more details, cf. Ref. [14]). Hence, we present only MSA results.

In our investigations we have studied the trends in the phase diagrams of such a system. Distinguishing between internal parameters (*i.e.* parameters that characterize the fluid–fluid interactions) and external parameters (*i.e.* parameters that characterize the matrix and the matrix–fluid interactions) we found that, similar as in the case of the bulk fluid, one can produce – for a given matrix density – trends in the types of phase diagram by varying the internal parameters. However, it is surprising that such trends can also be induced by varying the external parameters, keeping the internal parameters fixed.

The System and the Theoretical Methods

The System

The liquid chosen for this study is a symmetric binary mixture: the like-particle potentials (the components are denoted by indices '1' and '2') are identical ($\Phi_{11}(r) = \Phi_{22}(r)$), whereas the interaction between unlike particles, $\Phi_{12}(r)$, is different and is related to $\Phi_{ii}(r)$ *via* $\Phi_{12}(r) = \alpha\Phi_{ii}(r)$. This choice restricts the number of system parameters of a binary mixture drastically and simplifies systematic investigations. Nevertheless, a rich phase behaviour is to be expected. For $\Phi_{ij}(r)$ we have chosen hard-core *Yukawa* (HCY) potentials:

$$\beta\Phi_{ij}(r) = \begin{cases} \infty & \forall\ r \le \sigma \\ -\frac{K_{ij}}{r}\exp(-z(r-\sigma)) & \forall\ r > \sigma \end{cases} \tag{1}$$

The screening length z and the hard-sphere diameter σ are assumed to be equal for all potentials, whereas the interaction strengths are given by $K_{11} = K_{22}$ and $K_{12} = \alpha K_{11}$. Further system parameters are the concentrations of the two species of the fluid, $x_1 \equiv x$ and $x_2 = 1 - x_1$, and the number density of the fluid $\rho_f = \rho_1 + \rho_2$, ρ_i being the partial densities.

We then bring this binary fluid in contact with a disordered porous matrix. This matrix is assumed to be obtained by rapidly quenching a liquid configuration of matrix particles (index "0"), which are then immobile and not affected by the fluid particles; they interact with the fluid particles *via* potentials $\Phi_{0i}(r)$, $i = 1, 2$. For simplicity, the matrix particles have the same size as the fluid particles, and again a HCY potential is assumed for $\Phi_{0i}(r)$: the contact values K_{0i} are related to the fluid–fluid contact values *via* $K_{01} = K_{02} = yK_{11}$, and the number density of the matrix will be denoted by ρ_0. Further, we assume a pure hard-sphere matrix, *i.e.* $K_{00} = 0$.

We define a reduced temperature *via* $T^\star = \sigma/K_{11}$ (in the following, $T^\star$ is symbolized by T), and we put σ to unity. The reduced density is hence given by $\rho_f^\star = \sigma^3 \rho_f = \rho_f$.

Theoretical Methods

Liquid state theory for the bulk fluid

The structural and thermodynamic properties of the system have been calculated with methods based on statistical mechanics. The systems are assumed to be homogeneous and isotropic; hence, the correlation functions that describe the structure of the system depend on the distance of the particles only. The central correlation function in our approach is the so-called pair distribution function (PDF), $g(r)$. It is a function of the distance r between two particles and depends on temperature, density, and the interatomic potential. The PDF measures the extend to which the structure of a fluid deviates from complete randomness. Let us assume that we pick out one particle of the fluid and move with this particle through the volume that is occupied by the fluid. Counting at each time-step the number of particles separated by a distance r from this particle, we find that $4\pi\rho g(r) r^2 dr$ is the mean number of particles in a spherical shell of thickness dr and radius r. Since the fluid particles become uncorrelated for large distances, $\lim_{r\to\infty} g(r) = 1$. One then introduces the total correlation function *via* $h(r) = g(r) - 1$. The direct correlation function, $c(r)$, is defined *via* the *Ornstein-Zernike* (OZ) equation [10] *via*

$$h(r) = c(r) + \rho \int c(r') h(|\mathbf{r} - \mathbf{r}'|) d^3 r' \tag{2}$$

which expresses that the total correlation between two particles separated by a distance r is given by the direct correlation between these particles plus the indirect correlation, mediated *via* an arbitrary number of other particles in the fluid and expressed by the convolution integral in Eq. (2). For a broader overview over correlation functions we refer to [11].

In the binary cases these correlation functions are generalized to sets of correlation functions, introducing pairs of indices (ij) with $i, j = 1, 2$ and indicating correlations between particles of species i and j. These functions are denoted by $g_{ij}(r)$, $h_{ij}(r)$, and $c_{ij}(r)$. The OZ equations (now a set of three coupled integral-equations) read

$$h_{ij}(r) = c_{ij}(r) + \sum_{k=1,2} \rho_k \int c_{ik}(r') h_{kj}(|\mathbf{r} - \mathbf{r}'|) d^3 r' \quad i,j = 1,2. \tag{3}$$

For a given set of $h_{ij}(r)$, the OZ equations can be viewed as defining relations for the direct correlation functions $c_{ij}(r)$. However, in general, both sets of correlation functions are unknown. In order to make a solution of the OZ equations possible, a further relation between these sets of functions and the set of pair potentials, $\Phi_{ij}(r)$, has to be provided; such a (functional) relation is called a closure relation and can formally be written as $F(\{c_{ij}\}, \{h_{ij}\}, \{\Phi_{ij}\}) = 0$. Closure relations are derived from exact expressions of statistical mechanics using simplifying assumptions. Since the pair distribution functions $g_{ij}(r)$ obtained with these (approximate) methods are not

exact for a given set of pair potentials $\Phi_{ij}(r)$, this leads to an effect that is known in the literature as thermodynamic inconsistency which will be discussed later. A considerable number of such closure relations have been used in the literature during the past years; for an overview, see Refs. [11, 15]. The closure relations employed here are the mean spherical approximation (MSA) [11, 15] and the self-consistent *Ornstein-Zernike* approximation (SCOZA) [12]; they will be discussed in the subsequent subsections.

Once the structure is known in terms of the correlation functions, the thermodynamic properties can be calculated in a straightforward way. To this end, statistical mechanics provides different routes, such as the energy, the virial, or the compressibility route. In the energy route, the excess (over ideal gas) internal energy U^{ex} is given by

$$\frac{U^{\mathrm{ex}}}{V} = u = 2\pi \sum_{ij} \rho_i \rho_j \int \Phi_{ij}(r) g_{ij}(r) r^2 dr \tag{4}$$

where V is the volume of the system. In the virial route, the pressure P is calculated *via*

$$\beta P = \rho - \frac{2\pi}{3} \beta \sum_{ij} \rho_i \rho_j \int \Phi'_{ij}(r) g_{ij}(r) r^3 dr \tag{5}$$

(the prime stands for the derivative of the potentials with respect to the distance). Finally, the compressibility route relates the isothermal compressibility, $\chi_T = (-1/V)(\partial V/\partial P)_T$, to the zero-$q$ limit of the direct correlation functions *via*

$$\frac{\beta}{\rho \chi_T} = \frac{1}{\chi_T^{\mathrm{red}}} = 1 - \frac{1}{\rho} \sum_{ij} \rho_i \rho_j \tilde{c}_{ij}(q = 0) \tag{6}$$

where the tilde represents a three-dimensional *Fourier* transform. Further thermodynamic quantities relevant for the determination of phase equilibria (such as the free energy A or the chemical potentials μ_i, $i = 1, 2$) can be derived from the above quantities *via* thermodynamic integration or differentiation (using an appropriately chosen *Maxwell* relation).

If the structure functions were exact for the given system, one should obtain the same results for the thermodynamic properties *via* each of these three routes; the system is then called thermodynamically self-consistent. Computer simulations are one of the few methods that – apart from size-effects – provide self-consistent results. If approximations are introduced in the calculation of the correlation functions (and this is certainly the case when using closure relations), the different routes will lead to different results for the thermodynamic properties; the method is then called thermodynamically inconsistent.

Given the thermodynamic properties, one can then determine the coexistence parameters of two (or more) coexisting phases (denoted by Greek indices). These parameters are calculated from the coexistence relations which, for a given temperature T, read

$$P^{\alpha}(\rho^{\alpha}, x_1^{\alpha}) = P^{\beta}(\rho^{\beta}, x_1^{\beta}) \tag{7}$$

and

$$\mu_i^{\alpha}(\rho^{\alpha}, x_1^{\alpha}) = \mu_i^{\beta}(\rho^{\beta}, x_1^{\beta}) \quad (i = 1, 2). \tag{8}$$

For a general binary mixture, up to four phases can coexist.

Liquid state theory for a fluid in contact with a porous matrix

The route outlined above for a bulk fluid and leading from the set of interactions to the thermodynamic properties of a system is considerably more complex in the case where the fluid is in contact with a porous matrix. In our investigations the matrix is obtained by a thermal quench of an equilibrated liquid configuration (matrix particles carry the index '0'). Hence, our system represents a very special three-component fluid: the particles of the matrix are assumed to be fixed in place and are not affected by the mobile particles of the fluid, whereas the fluid particles are allowed to equilibrate in the rigid matrix structure. Physical quantities are therefore obtained by two successive averages: a first average is taken over the degrees of freedom of the fluid particles (keeping the positions of the matrix particles fixed), and a second average is taken over all possible degrees of freedom of the matrix particles. Perhaps the most promising approach to solve this problem has been proposed by *Given* and *Stell* [13] who have introduced the replica trick [16] in this field: it exploits an isomorphism between the partly quenched and a fully equilibrated fluid mixture (the so-called replicated system) which consists of the now mobile matrix particles and of s noninteracting identical copies of the liquid. The properties of the partly quenched system are obtained by considering the limit $s \to 0$ of the properties of the equilibrium system which, in turn, can be treated by standard liquid state theories (see preceding subsection). Applying this framework for our system, nine OZ-type integral equations [14] (so-called replica *Ornstein-Zernike* equations, ROZ) can be derived that relate the direct and total correlation functions of the fluid and of the matrix particles. One of these equations describes the matrix correlation functions and is decoupled from the other equations; the remaining eight equations are coupled. Again, they have to be solved along with a closure relation.

In a similar way one can calculate the thermodynamic properties of the replicated system (using the standard relations mentioned in the preceding section) and then apply the limit $s \to 0$. In this manner, thermodynamic relations corresponding to Eqs. (4)–(6) are obtained which are considerably more complicated and are therefore not reproduced here; for details, see Ref. [14]. The phase equilibrium between coexisting phases is again calculated by equating the pressure and the chemical potentials for a given temperature T.

The mean spherical approximation

The closure relation of the mean spherical approximation (MSA) is given by [11]

$$g_{ij}(r) = 0 \quad (r < \sigma = 1) \tag{9}$$

and

$$c_{ij}(r) = -\beta \Phi_{ij}(r) \quad (r > \sigma = 1). \tag{10}$$

Whereas the first relation is – due to the impenetrability of the particles – exact, the second relation represents an approximation: one assumes that the long-distance behaviour of the direct correlation functions (*i.e.* $c_{ij}(r) \rightarrow -\beta\Phi_{ij}(r)$ for $r \rightarrow \infty$) is valid for all distances. As a consequence, the MSA leads to thermodynamically inconsistent data for the thermodynamic properties. Nevertheless, as will be shown in subsequent sections, it provides qualitatively good results in comparison with computer simulation data for systems not too close to phase boundaries or to a critical region.

The self-consistent Ornstein-Zernike approximation

The self-consistent *Ornstein-Zernike* approximation (SCOZA) was introduced in its original version [12] by *Høye* and *Stell* and has been refined ever since: meanwhile, it exists in several versions of different levels of sophistication (for an overview, Ref. [17]). The aims of the SCOZA are two-fold: first, it overcomes the lack of thermodynamic inconsistency of the MSA by imposing thermodynamic consistency between the energy and the compressibility route; second, the SCOZA is well-suited to treat fluids near phase transitions and near criticality accurately.

We present here the formulation of the SCOZA in its simplest version (for the more sophisticated versions, cf. Ref. [17]); the closure relations now read

$$g_{ij}(r) = 0 \quad (r < \sigma = 1) \tag{11}$$

and

$$c_{ij}(r) = K_{ij}(\rho, \beta, x)\Phi_{ij}(r) \quad (r > \sigma = 1). \tag{12}$$

A comparison with the MSA closure relations shows that the state-dependent functions $K_{ij}(\rho, \beta)$ replace the prefactor $-\beta$ in Eq. (10). We use the simplifying assumption that $K_{ij}(\rho, \beta, x) = K(\rho, \beta, x)$. In contrast to the MSA, where $K(\rho, \beta, x) = -\beta$, this function is not known *a priori* but is determined in the SCOZA by imposing consistency between the energy and the compressibility route, *i.e.* u (determined *via* the energy route) and χ_T^{red} (calculated *via* the compressibility route) have to fulfill the following partial differential equation (PDE):

$$\rho \frac{\partial^2 u}{\partial \rho^2} = \frac{\partial}{\partial \beta}\left(\frac{1}{\chi_T^{\text{red}}}\right). \tag{13}$$

Equation (13) supplemented with the OZ equation (Eq. (3)), the closure relations (Eqs. (11) and (12)), and Eqs. (4) and (6) represents a partial differential equation for $K(\rho, \beta, x)$, which is transformed (*via* a rather complex and heavy formalism) into a (diffusion-type) PDE for u with a known function $B(\rho, u)$:

$$B(\rho, u)\frac{\partial u}{\partial \beta} = \rho \frac{\partial^2 u}{\partial \rho^2} \tag{14}$$

The steps from Eq. (13) to Eq. (14) are based on the fact that the OZ-equations supplemented by the closure relations *vide supra* can be solved *semi*-analytically for a HCY-mixture [18–20]. Using these results, the formulation of the SCOZA

can be derived in a rather straightforward (but cumbersome) way. The numerical implementation is very demanding.

This simplifying fact represents a considerable advantage for the system investigated here. However, it also points out the main drawback of the SCOZA: its application is restricted (at least up to now) to such systems where a basic analytic concept is available. Hence, it is not surprising, that the SCOZA has been solved up to now only for HCY-systems and for the lattice gas model [21]. In a more general case, where such a (*semi*-)analytic help is not available, all calculations have to be performed numerically.

Results

Bulk Fluid

Phase diagrams

In the first part of this study we have investigated the phase diagram of the pure binary symmetric mixture defined in the preceding section. For the interaction parameter α, which characterizes the ratio between the unlike and the like interactions, we have chosen values smaller than one. This guarantees, that, apart from the vapour–liquid transition, we shall also encounter a fluid–fluid decomposition for a sufficiently small α. We expect the following phases: a homogeneous (equimolar) gas (G), a homogeneous (equimolar) liquid (L), and a nonequimolar (demixed) fluid (DF). The solid phases have not been considered here.

In some of the figures we shall present the MSA data; several of these are supplemented by results from grand canonical Monte-Carlo simulations performed by *D. Levesque* and *J.-J. Weis* [22] (for details of the simulation, see references in this paper). The phase diagrams presented are projections of the three dimensional (T, ρ, x) phase diagram onto the $(x = 1/2)$ plane. In Fig. 1, such a three-dimensional presentation is shown; the phase diagram is of type II (see below).

In a first step we have applied the (simple and thermodynamically inconsistent) MSA (Eqs. (9) and (10)). The results are shown in Fig. 2 for five different α-values. One can clearly follow the strong influence of the parameter α: for $\alpha = 0.9$ we observe a coexistence between the G and the L phases. There is probably no fluid-fluid phase separation: the existence of a DF phase and the corresponding transition is characterized in these figures by the so-called λ-line, the critical line of the fluid–fluid demixing transition: for a given temperature T, the critical density for this demixing transition is given by $\rho_c(T)$; these values of $\rho_c(T)$ represent the λ-line as a function of T. For densities larger than $\rho_c(T)$ we observe the DF phase, whereas for densities smaller than $\rho_c(T)$ we encounter the equimolar phase. As we decrease α, this λ-line approaches the G-L coexistence line from the high-density side and intersects this first order transition in a so-called critical end point (CEP); here, a non-critical vapour coexists with a critical nonequimolar (demixed) fluid (DF). Such a phase diagram will be called a type I phase diagram. Below the CEP temperature one observes a triple line where a vapour coexists with a 1-rich and a 2-rich fluid. By further decreasing α, the λ-line intersects the G-L coexistence curve at temperatures close to the G-L critical point, leading to a so-called

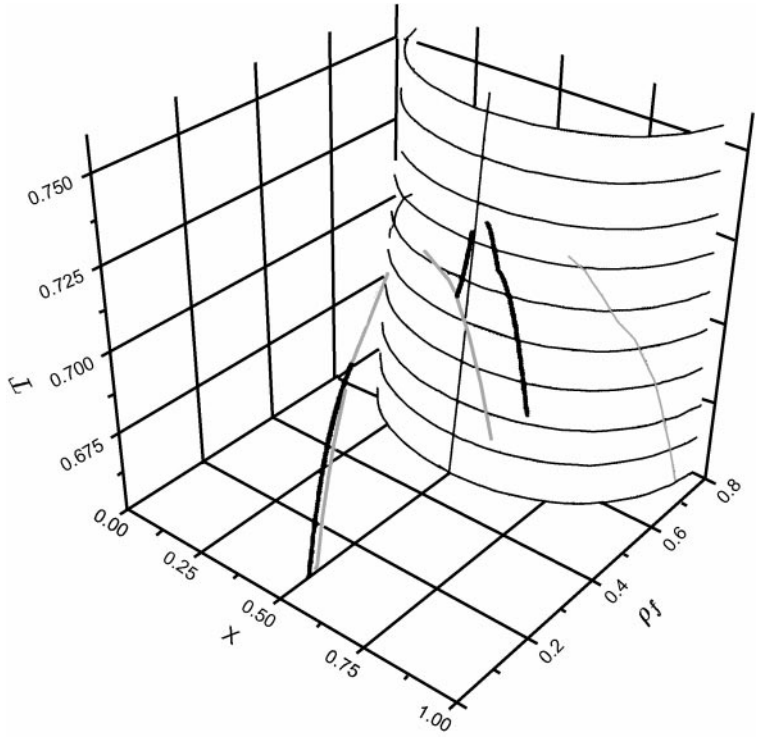

Fig. 1. Phase diagram of a binary bulk mixture in (T, ρ_f, x)-space; the curves in the ($x = 1/2$) plane represent the phase diagram that will be presented in the following figures (thick black and grey lines); demixing transitions are depicted for several isothermal planes by the thin grey lines in the high density regime; the critical points of this demixing transition are connected by the λ-line; from Ref. [23]

tricritical point: here L and DF become critical simultaneously, characterized by two vanishing order parameters; such a phase diagram is denoted to be of type II. We also observe a point where four phases (L, G, 1-rich DF, 2-rich DF) coexist. In addition, we encounter in phase diagrams of type I and II the usual critical point of the G-L phase coexistence. Finally, upon further decreasing α we observe the type III phase diagram, where the G-L transition is completely suppressed. Again we obtain a tricritical point where the L and the DF phase become simultaneously critical. Apart from the stable phase transitions we have also depicted in these figures the metastable phase equilibria; they are of relevance for the dynamic properties of the system (for a more detailed discussion, see Refs. [2, 22]). A comparison with computer simulations shows that the MSA gives reasonably good results for the bulk case.

Stability

The *semi*-analytic character of the SCOZA formalism offers the possibility to study the stability of our system in detail. As shown in Ref. [20], the mechanical stability (*i.e.* with respect to L-G separation) and the chemical stability (*i.e.* with respect to the demixing transition) can be studied using the *semi*-analytical expressions of the

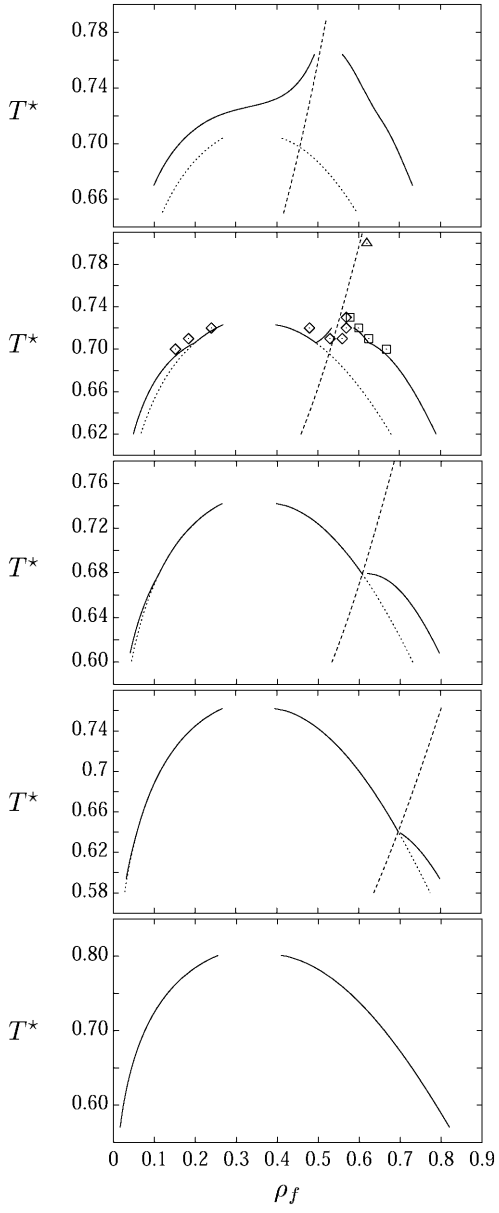

Fig. 2. Variation of α of the phase diagram of the binary symmetric bulk mixture from MSA: $\alpha = 0.65$, 0.70, 0.75, 0.80, and 0.90 (from top to bottom); full line: G-L, G-DF, or L-DF coexistence curves; dotted line: metastable G-L transition; dashed line: λ-line; symbols: grand canonical Monte Carlo simulations from Ref. [22]

MSA formalism. In Fig. 3 we depict this border, which in (T, ρ, x)-space is a surface: above this surface, the system is stable, whereas below it is unstable. The mechanical instability is expressed by a divergence of χ_T^{red}: it is encountered only along the $(x = 1/2)$ line on this surface. The onset of the chemical instability, on the other hand, is characterized by a change in the sign of $(\partial^2 G/\partial x^2)$, where G is the *Gibbs* free energy [15].

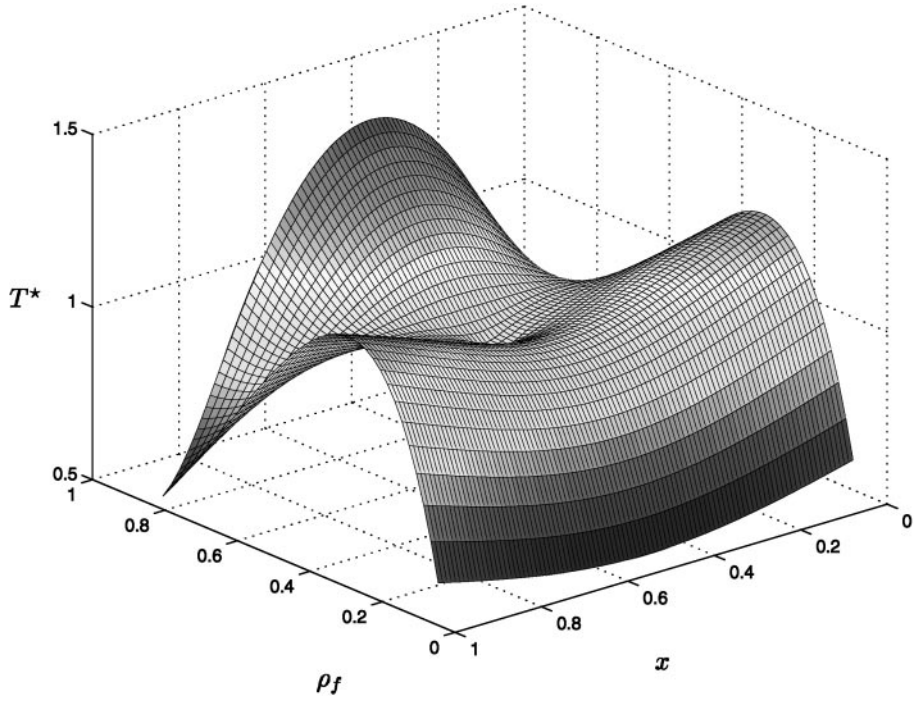

Fig. 3. Surface separating the stable (above) from the unstable (below) states of a symmetric binary bulk fluid in (T, ρ_f, x) – space ($z\sigma = 1.8$, $\alpha = 0.65$); see text

Fluid in a Porous Matrix

We have now brought our bulk fluid in thermal equilibrium with a porous matrix. Four parameters can be varied: (*i*) α, the ratio between unlike and like fluid particle interactions, (*ii*) y, the ratio between the matrix–fluid interactions and the potential of the like fluid particles: positive and negative values of y correspond to attractive and repulsive matrix–fluid interactions, (*iii*) the matrix density ρ_0 and (*iv*) the screening length z of the potentials. In an effort to enable a comparison with the computer simulations we have truncated our HCY-potentials (unless otherwise stated) at a cut-off radius of $r_c = 2.5\ \sigma$.

Comparison with simulations

We have first compared the MSA data with simulation results. The computer simulations were carried out for four different matrix densities $\rho_0 = 0$, 0.05, 0.15, and 0.3 at $\alpha = 0.7$, $y = 1$, $z\sigma = 2.5$, and $r_c = 2.5\ \sigma$ (for technical details, see Ref. [22] and references quoted therein). The results are shown in Fig. 4. For $\rho_0 = 0$ one observes a type II phase diagram: a first order G-L transition with a critical temperature of $T_c \approx 0.72$–0.73 and a critical density $\rho_c \approx 0.35$ and a line of second order demixing transitions terminating at a tricritical point with a temperature of $T_{tc} \approx 0.73$, slightly higher than the critical temperature, and a density of $\rho_{tc} \approx 0.57$. As we increase the matrix density, the temperature range within which the equimolar liquid exists decreases, and the phase diagram becomes a type I

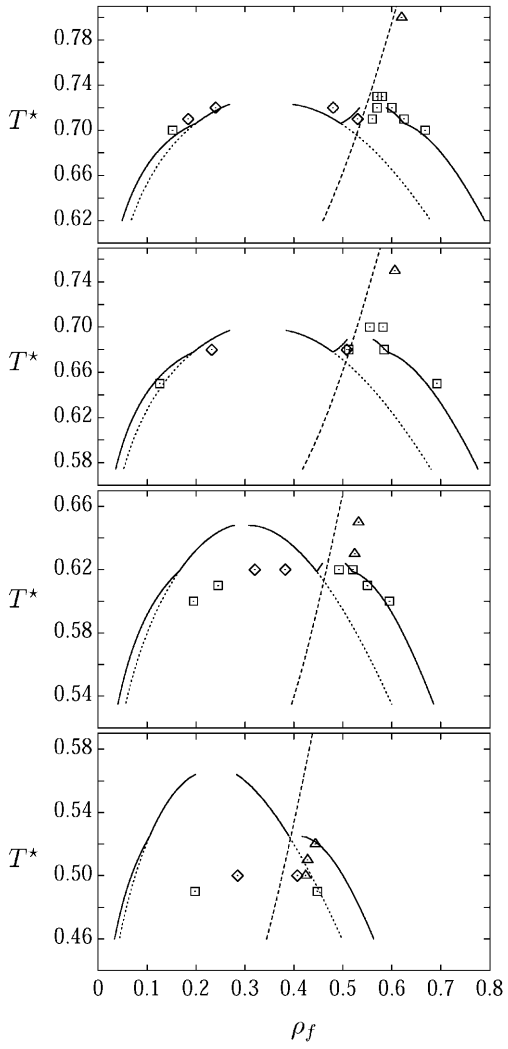

Fig. 4. Variation of the phase diagram of a binary fluid mixture in contact with a porous matrix with matrix density ρ_0 ($\alpha = 0.7$, $y = 1$, $z\sigma = 2.5$): comparison between grand canonical Monte Carlo (GCMC) and MSA results; $\rho_0 = 0$, 0.05, 0.15, and 0.30 (from top to bottom); symbols: GCMC simulations (diamonds: G-L equilibrium; squares: G-DF or L-DF equilibrium; triangles: λ-line); lines: MSA results (full line: G-L, G-DF or L-DF coexistence curve; dotted line: metastable G-L transitions; dashed line: λ-line); from Ref. [22]

diagram. At $\rho_0 = 0.3$ the phase diagram reveals (within accuracy of the simulation results) a tricritical point in the temperature range 0.49–0.52, or possibly a critical end point.

Although the trends in the types of phase diagrams are reproduced qualitatively in the simulations, it becomes obvious from Fig. 4 that the quantitative agreement between MSA data and simulation results deteriorates as we increase the matrix density: whereas for the pure bulk fluid ($\rho_0 = 0$) we have excellent agreement (both for the two first-order transitions and for the position of the λ-line), marked differences between these two sets of data appear as the matrix density increases.

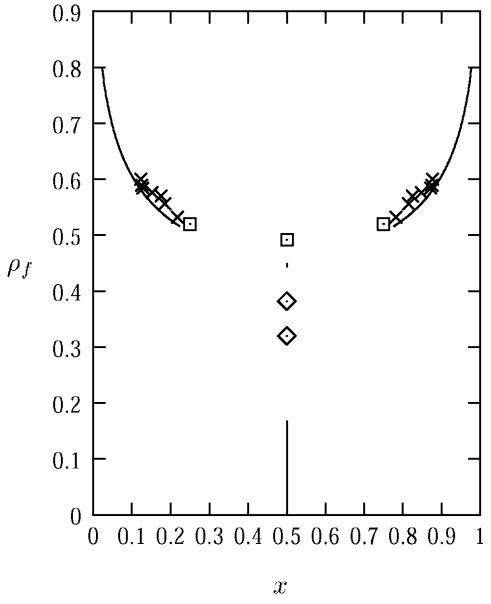

Fig. 5. Demixing transition of a binary fluid in contact with a porous matrix of density $\rho_0 = 0.15$ ($\alpha = 0.7$, $y = 1$, $z\sigma = 2.5$): ρ_f as a function of concentration x for $T = 0.62$; the symbols denote GCMC simulations (diamonds: G-L equilibrium; squares: L-DF equilibrium; crosses: first order demixing transition), the lines MSA results; from Ref. [17]

The critical temperatures obtained in the simulations are considerably lower than for the MSA data, whereas the critical densities are shifted to higher values. In addition, Fig. 5 shows the demixing transition for one of the systems: these phase diagrams are horizontal (isothermal) cuts through the three-dimensional phase diagram of Fig. 1. It is surprising, that – in contrast to the phase diagrams presented in Fig. 4 (projections onto the ($x = 1/2$) plane) – the concentrations of the demixed phase agree very nicely with simulation data even at high matrix densities. It is obvious that these differences are due to deficiencies of the MSA.

Variation of α

The variation of the phase diagram with α (ratio of the interaction strengths between unlike and like particles) is shown in Fig. 6 for a matrix density of $\rho_0 = 0.1$. $z\sigma$ was chosen to be 2.5; variation of this parameter for the bulk fluid was already discussed before. In an effort to study in addition the influence of the matrix–fluid interaction we have considered a pure hard sphere ($y = 0$) and a HCY ($y = 1$) matrix–fluid interaction. Although qualitatively the sequence of types of phase diagrams is the same in the two series (type III $\rightarrow$ type II $\rightarrow$ type I), the character of the matrix–fluid interaction leads to quantitative changes: keeping the matrix density fixed to $\rho_0 = 0.1$, the change of y from 1 to 0 (*i.e.* from an attractive HCY interaction to a pure hard sphere matrix) lowers T_c by *ca.*10%, shifts ρ_c from $\sim$0.32 to $\sim$0.26, and delays the appearance of the CEP as one increases α.

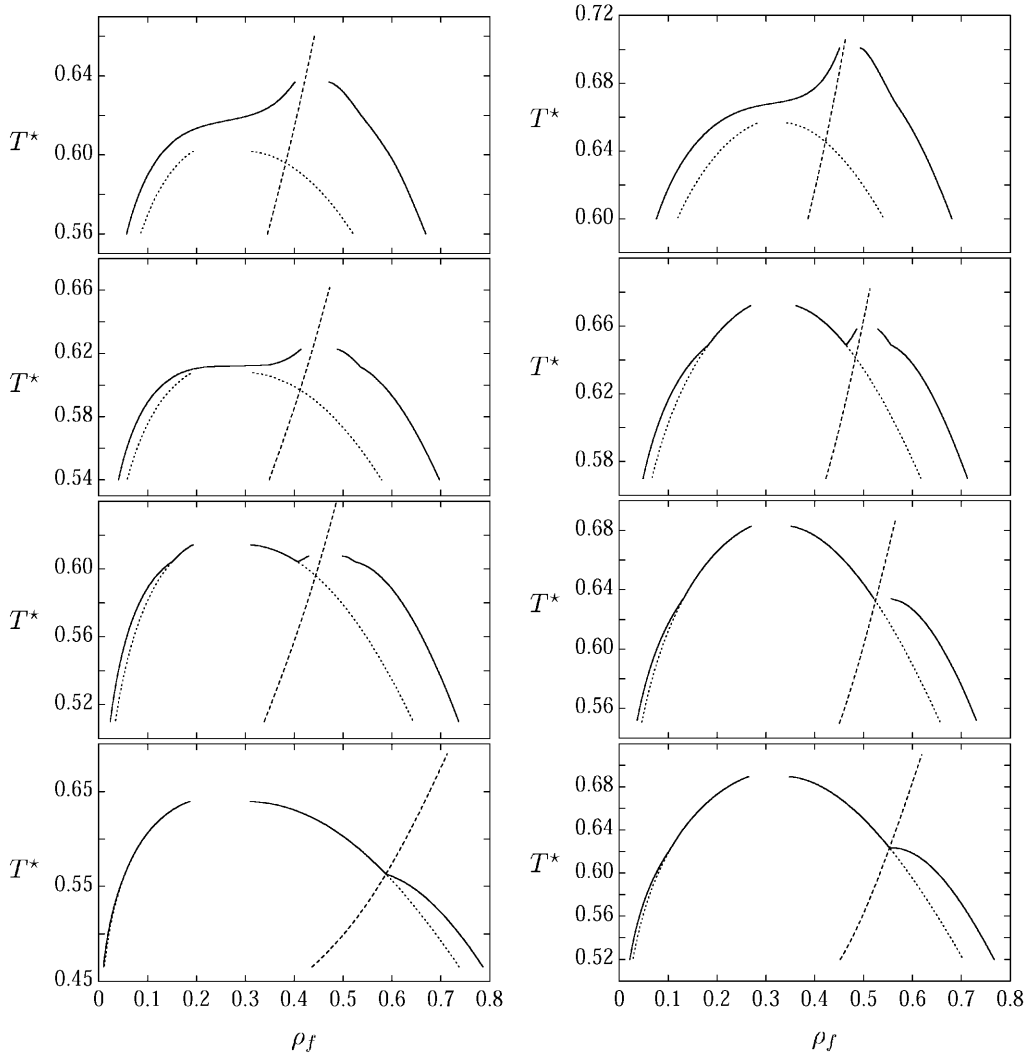

Fig. 6. Variation of the phase diagram of the binary fluid mixture in thermal equilibrium with a porous matrix from MSA with α; left column ($\rho_0 = 0.1$, $y = 0$): $\alpha = 0.68$, 0.70, 0.72, and 0.80 (from top to bottom); right column ($\rho_0 = 0.1$, $y = 1$): $\alpha = 0.65$, 0.70, 0.73, and 0.75 (from top to bottom); full line: G-L, G-DF or L-DF coexistence curves; dotted line: metastable G-L transition; dashed line: λ-line; from Ref. [22]

Variation of y

The parameter y is the ratio between the fluid–fluid and the matrix–fluid interactions; $y > 0$ represents an attraction between matrix and fluid particles, whereas $y < 0$ represents a repulsion. The influence of y on the phase behaviour is shown in Fig. 7 for two different pairs of (ρ_0, α) with $z\sigma = 2.5$: (*i*) $\rho_0 = 0.05$, $\alpha = 0.7$; (*ii*) $\rho_0 = 0.1$, $\alpha = 0.73$. For the lower matrix density, $\rho_0 = 0.05$, the sequence of phase diagrams is found to be type III $\rightarrow$ type II $\rightarrow$ type III when y decreases from positive to negative values. A G-L transition appears near $y \sim 2$ (a precise location cannot be found due to numerical problems in the critical region as

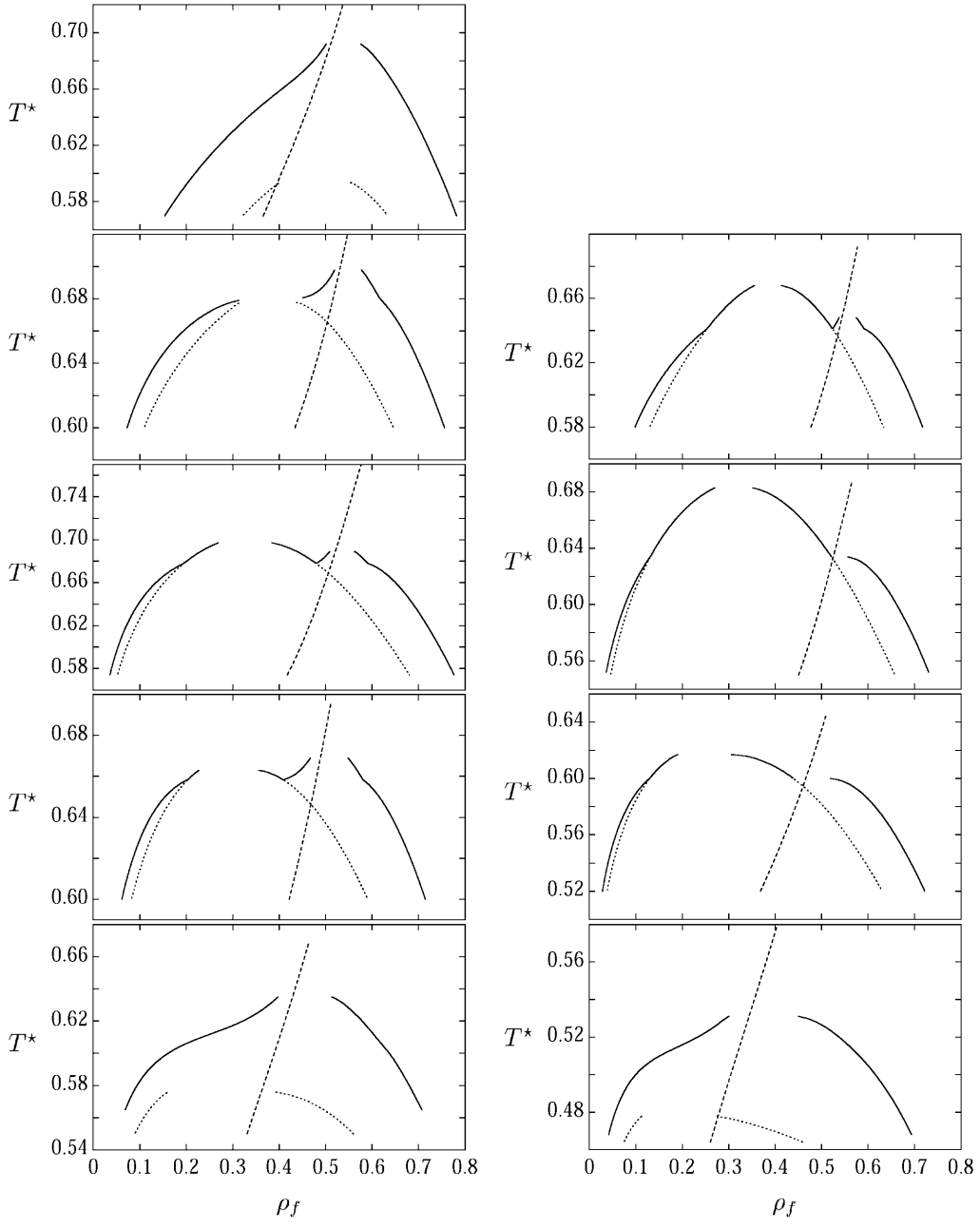

Fig. 7. Variation of the phase diagram of the binary fluid mixture in thermal equilibrium with a porous matrix from MSA with y; left column ($\rho_0 = 0.05$, $\alpha = 0.7$): $y = 3.5$, 2, 1, 0, -1 (from top to bottom); right column ($\rho_0 = 0.10$, $\alpha = 0.73$): $y = 2$, 1, 0, -1 (from top to bottom); full line: G-L, G-DF, or L-DF coexistence curves; dotted line: metastable G-L transition; dashed line: λ-line; from Ref. [22]

mentioned above) and exists only in a small range of y-values, extending roughly from 2 to -0.5. The phase diagram is again of type III for the more strongly repulsive matrix–fluid interaction $y = -1$. The matrix density has only a minor influence on the qualitative sequence of the types of phase diagrams: for the

larger matrix density $\rho_0 = 0.1$, the type II phase behaviour occurs at least for $0 < y < 2$.

Variation of ρ_0

The influence of the matrix density ρ_0 on the phase diagram of the mixture is shown in Fig. 8 for two values of the parameter y ($y = 0$ and 1) and $\alpha = 0.7$; we assume $z\sigma = 2.5$. As discussed in the comparison of simulation and theoretical results, in both cases we have a type II diagram characterized by a tricritical point

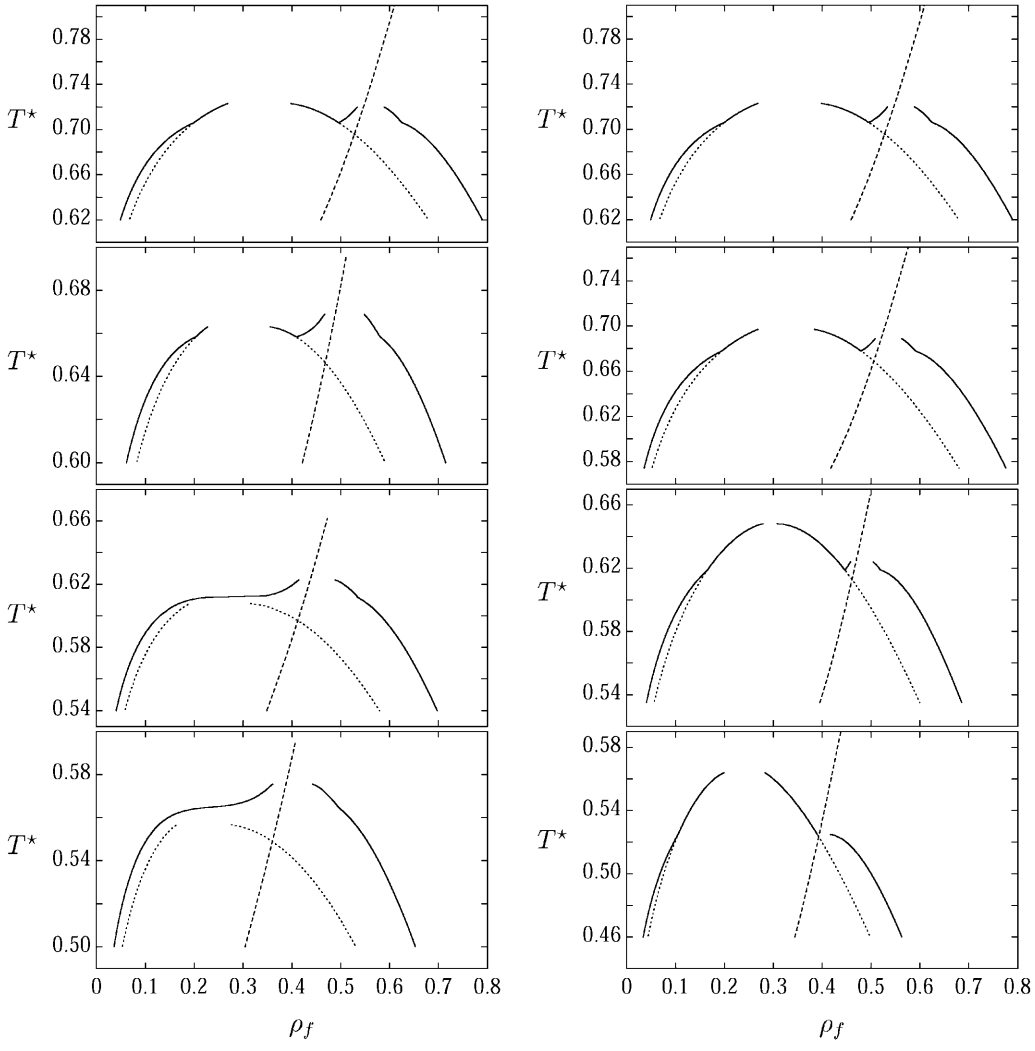

Fig. 8. Variation of the phase diagram of the binary fluid mixture in thermal equilibrium with a porous matrix from MSA with matrix density ρ_0; left column ($y = 0$, $\alpha = 0.7$): $\rho_0 = 0$, 0.05, 0.10, and 0.15 (from top to bottom); right column ($y = 1$, $\alpha = 0.7$): $\rho_0 = 0$, 0.05, 0.15, and 0.30 (from top to bottom); full line: G-L, G-DF, or L-DF coexistence curves; dotted line: metastable G-L transition; dashed line: λ-line; from Ref. [22]

at $\rho_0 = 0$, where the λ-line of the second order demixing transition terminates, as well as a triple point where G, L, and DF coexist. As we increase ρ_0, at $y = 1$ (attractive tail in the matrix–fluid interaction) the tricritical temperature T_{tc} decreases; at $\rho_0 \sim 0.3$ the first order transition between L and DF has vanished, giving rise to a CEP at T_{cep} (type I phase diagram). It can be noted that the existence of a CEP leads to a kink in the G-L curve, clearly visible in the MSA data, a phenomenon which has been discussed in a simulation study of the pure mixture [24]. It is rather surprising that for the case of a pure hard sphere matrix–fluid interaction ($y = 0$) a different scenario is observed: increasing ρ_0 now leads to a type III phase diagram; for $\rho_0 \sim 0.1$ the G-L transition becomes metastable and hidden below the G-DF transition (type III phase diagram). This points out very nicely the strong influence of the matrix (external system parameter) on the phase behaviour of the fluid.

Variation of z

Finally, we have varied the screening length z of the potential. Since its influence is less dramatic than any of the other system parameters, we do not present a figure but rather summarize the results: variation of the screening length $z\sigma$ from 2 to 3 lowers the tricritical temperature and the critical temperature of the metastable G-L transition; the type of the phase diagram is unaffected.

Conclusions

In this contribution we have discussed the phase behaviour and the criticality of a binary fluid mixture, restricting ourselves to a symmetric binary fluid. Here the potentials between the like particles are equal, but differ, on the other hand, from the unlike interactions; the attraction between particles of different species is assumed to be weaker than the like particle interaction. We have first considered the case of the binary bulk fluid and have calculated structural and thermodynamic properties *via* the simple (and thermodynamically inconsistent) MSA and the sophisticated (and thermodynamically self-consistent) SCOZA models. We have seen – leaving the solid phases aside – three coexisting phases: the equimolar gas (G), the equimolar liquid (L), and the nonequimolar (demixed) fluid (DF). As a consequence of the symmetry of the system we encounter three types of phase diagrams that are characterized by the different loci where the λ-line (*i.e.* the line of critical points of the DF transition) intersects the second order G-L transition. We show by using the simple MSA that the three types of phase diagram are induced by the parameter that measures the strength of the unlike interaction. The SCOZA helps us to get more quantitative results: we have calculated critical points and have given a stability analysis (both with respect to mechanical as well as to chemical stability). We then immerse this symmetric binary mixture in a porous matrix, realized by a frozen configuration of a liquid. Structural and thermodynamic quantities are again calculated from liquid state theory; however, one has to apply a special trick (replica trick) to take into account the fact that in this special ternary mixture (binary liquid + matrix) the matrix particles interact with the liquid particles, but are assumed to be immobile: there is no structural response

of the fluid to the matrix. Here we have used only MSA to calculate the properties of the fluid. By systematically varying the system parameters we have shown that the trends between the three types of phase diagrams are not only triggered by the internals system parameters (*i.e.* the parameters that characterize the fluid), but also by varying the external parameters (*i.e.* the matrix properties and the interaction fluid–matrix). This might be of relevance for technological applications (catalysis, adsorption, *etc.*) where the phase behaviour of the fluid can be influenced by varying the (chemical) properties of the matrix. Extension of this concept by considering fluids with orientational interactions (dipolar and molecular fluids) and charged particles is currently in progress and will be presented in due course.

Acknowledgments

This work was supported by the *Österreichische Forschungsfonds* under Project Nos. P13062-TPH and P14371-TPH and the *Wiener Handelskammer. E. Schöll-Paschinger* is a student of the Graduate Program ''Computational Material Science'' of the *Österreichische Forschungsfonds* (Proj. No. W004). The authors are indebted to Profs. *D. Levesque* and *J.-J. Weis* at the Laboratoire de Physique Théorique (Université Paris-Sud, Orsay) for providing computer simulation data and for many stimulating discussions.

References

[1] van Konynenburg HP, Scott RL (1980) Philos Trans R Soc Ser A **298**: 495
[2] Wilding NB, Schmid F, Nielaba P (1998) Phys Rev E **58**: 2201.
[3] Rosinberg M-L (1999) In: Caccamo C, Hansen J-P, Stell G (eds) New Approaches to Problems in Liquid State Theory. NATO Science Series, Kluwer, Dordrecht
[4] Wong APY, Chan MHW (1990) Phys Rev Lett **65**: 2569; Wong APY, Kim SB, Goldburg WI, Chan MHW (1993) Phys Rev Lett **70**: 954; Chan M, Mulders N, Reppy J (1996) Physics Today **49**: 30
[5] Kim SB, Ma J, Chan MHW (1993) Phys Rev Lett **71**: 2268; Tulimieri DJ, Yoon J, Chan MHW (1999) Phys Rev Lett **82**: 121 and references therein.
[6] See e.g. Frisken BJ, Ferri F, Cannell DS (1995) Phys Rev E **51**: 5922 and references therein; Zhuang Z, Casielles AG, Cannell, DS (1996) Phys Rev Lett **77**: 2969; Maher JV, Goldburg WI, Pohl DW, Lanz M (1984) Phys Rev Lett **53**: 60
[7] See e.g. Goh MC, Goldburg WI, Knobler CM (1987) Phys Rev Lett **58**: 1008; Dierker SB, Wiltzius P (1987) Phys Rev Lett **58**: 1865; Wiltzius P, Dierker SB, Dennis BS (1989) Phys Rev Lett **62**: 804; Dierker SB, Wiltzius P (1991) Phys Rev Lett **66**: 1185; Aliev F, Goldburg WI, Wu X-l (1993) Phys Rev E **47**: 3834 Lin MY, Sinha SK, Drake JM, Wu X-l, Thiyagarajan P, Stanley HB (1994) Phys Rev Lett **72**: 2207; Lacelle S, Tremblay L, Bussière Y, Cau F, Fry CG (1995) Phys Rev Lett **74**: 5228; Tulimieri DJ, Yoon J, Chan MHW (1999) Phys Rev Lett **82**: 121; Formisano F, Teixeira J (2000) Eur Phys J E **1**: 1
[8] Weis J-J, Nijmeijer MJP, Tavares JM, Telo da Gama MM (1997) Phys Rev E **55**: 436; Tavares JM, Telo da Gama MM, Teixeira PIC, Weis J-J, Nijmeijer MJP (1995) Phys Rev E **52**: 1915.
[9] Groh B, Dietrich S (1994) Phys Rev Lett **72**: 2422; Groh B, Dietrich S (1999) In: Caccamo C, Hansen J-P, Stell G (eds) New Approaches to Problems in Liquid State Theory. NATO Science Series, Kluwer, Dordrecht
[10] Ornstein LS, Zernike F (1914) Proc Acad Sci (Amsterdam) **17**: 793
[11] Hansen J-P, McDonald IR (1986) *Theory of Simple Liquids*, 2nd edn. New York, Academic Press
[12] Høye JS, Stell G (1977) J Chem Phys **67**: 439; Høye JS, Stell G (1984) Mol Phys **52**: 1071; for an overview see: Pini D, Stell G, Wilding NG (1998) Mol Phys **95**: 483

[13] Given JA (1992) Phys Rev A **45**: 816; Given JA, (1992) J Chem Phys **96**: 2287; Given JA, Stell G (1994) Physica A **209**: 495
[14] Paschinger E, Kahl G (2000) Phys Rev E **61**: 5330
[15] Caccamo C (1996) Phys Rep **274**: 1
[16] Edwards SF, Anderson PW (1975) J Phys F **5**: 965; Edwards SF, Jones C (1976) J Phys A **9**: 1595
[17] Schöll-Paschinger E (2001) PhD Thesis, Technische Universität Wien
[18] Høye JS, Blum L (1977) J Stat Phys **16**: 399
[19] Arrieta E, Jedrzejek C, Marsh KN (1987) J Chem Phys **86**: 3607
[20] Arrieta E, Jedrzejek C, Marsh KN (1991) J Chem Phys **95**: 6806
[21] Dickman R, Stell G (1996) Phys Rev Lett **77**: 996 Pini D, Stell G, Dickman R (1998) Phys Rev E **57**: 2862
[22] Schöll-Paschinger E, Levesque D, Weis J-J, Kahl G (2001) Phys Rev E **64**: 11502
[23] Lang A, PhD Thesis, Technische Universität Wien
[24] Wilding NB (1997) Phys Rev Lett **78**: 1488; (1997) Phys Rev E **55**: 6624

Received June 27, 2001. Accepted July 2, 2001